PREPRINT

DETECTION AND EVALUATION OF ULTRASONIC WAVES USING SINGLE MODE OPTICAL FIBER

BY

J. A. GILBERT C. P. BURGER T. D. DUDDERAR
J. A. SMITH B. R. PETERS

PRESENTED AT THE
VI INTERNATIONAL CONGRESS ON
EXPERIMENTAL MECHANICS

PORTLAND, OREGON

JUNE 1988

AT&T
Bell Laboratories

The Detection and Evaluation of Ultrasonic Waves Using Single Mode Optical Fiber Interferometry

J. A. Gilbert[†] C. P. Burger[*] T. D. Dudderar[#]
J. A. Smith[*]
B. R. Peters[†]

ABSTRACT

A new nondestructive evaluation (NDE) technique employing noncontacting optical fiber interferometry was used to sense Rayleigh waves traveling along the surface of a steel test bar. Time domain measurements were used to successfully identify the position of a machined slot in the bar and frequency analysis was used to estimate its size. This approach has many potential applications in the ultrasonic evaluation of real flaws in structures with complex surface geometries.

Introduction

There are many advantages to combining conventional ultrasonic excitation/interrogation techniques with sophisticated fiber optic sensing systems for the nondestructive evaluation of flaws in a variety of complex and/or inaccessible structures. First, optical fiber sensors do not require mechanical coupling of the transducer to the surface of the test structure at the point of detection. This is a significant advantage over traditional piezoelectric transducer-based ultrasonic techniques which require mechanical contact and can be very difficult to apply to structures with complex surface geometries. Second, since the optical fiber components themselves have low mass, volume and stiffness, they can be adapted for rapid and automated manipulation, positioning, and scanning. Finally, it will be shown that, since they are noncontacting (no mass attached to the test surface at the sensing location) point (high spatial resolution) detectors an optical fiber sensor can accurately measure an ultrasonic (displacement) response without incurring any deleterious interactions with the interrogating acoustic wavefronts. This accuracy assures highly reliable measurement of the propagation characteristics of both transmitted and reflected acoustic waves, greatly facilitating meaningful signal analysis in both the time and frequency domains.

Interferometry

A number of investigators [1-10] have successfully demonstrated the use of interferometry as a tool for measuring the highly transient surface displacements associated with ultrasonic inspection procedures. These authors used either classical or holo-interferometric arrangements to obtain the necessary sensitivity at high frequencies. They achieved adequate resolution but their systems utilized what were essentially laboratory instruments – tools which were not readily adaptable to field applications. On the other hand, many fiber optic-based sensors have been designed to measure extremely small displacements encountered in quasi-static and low to intermediate frequency vibration studies [11-16]. Unfortunately, the combination of response time and sensitivity available with them were not, until now, good enough to permit the characterization of flaws in metals by spectral analysis. Fortunately, through the synthesis of high speed photoelectronics and laser based fiber optic interferometry, this is no longer the case.

* Texas A&M University, College Station, TX 77843
† University of Alabama-Huntsville, Huntsville, AL 35899.
# AT&T Bell Laboratories, Murray Hill, NJ 07974

This paper describes the configuration and operation of an elementary optical fiber interferometer (OFI) capable of carrying out remote measurements of Rayleigh waves (surface acoustic waves, also called R-waves) associated with the ultrasonic interrogation of a steel bar. As shown in Figure 1, the unspread output from a laser is split into two beams of equal intensity by a variable beam splitter. One of the beams is used to excite a single mode optical fiber, the other is wasted. A small percentage of the beam propagating down the optical fiber is internally (Fresnel) reflected at the output end and serves as the reference wave. The remainder of the light emerges from the output end of the optical fiber and is scattered by the diffusely reflecting surface of the steel bar. A small but detectable fraction of this scattered light is reflected back into the optical fiber to interfere with the internally reflected reference wave in its propagation back through the fiber. Upon exiting the optical fiber at the original input end, the returning light is collimated by the same lens used to originally launch the light into the fiber. Half of this collimated output beam is deflected by the beam splitter through an aperture and collecting lens onto one end of a multimode optical fiber which guides the light to a fast photodiode with custom wide band amplification electronics.

Naturally, since the OFI is excited by coherent light, if the optical path length of the externally reflected and recaptured light beam differs by a half wave length or odd multiple thereof (due to its travel across the sensing cavity to the test surface and back to the fiber tip) from the optical path length of the internally reflected reference beam, they will interfere destructively. On the other hand, if the difference is a whole wavelength or multiple thereof the interference will be constructive. So long as the intensities and polarizations of the two reflections are reasonably equal, the light output from the optical fiber will be seen to brighten and darken as the reflecting test surface moves towards (or away) from the optical fiber tip. A displacement induced change in cavity length of only one quarter of an optical wavelength is sufficient to shift the output signal intensity from a maximum to a minimum or vice versa.

In order to receive the maximum signal from the OFI, a translation stage is used to move the fiber tip linearly in and out from the specimen surface. This permits the operator to adjust the amount of light recaptured by the fiber tip and thereby match the intensity of the internally reflected reference wave. In the present tests on moderately reflective machined steel surfaces, acceptable results were obtained with cavity lengths (or standoff distances) as long as 1 mm and as short as none.

One important feature of the OFI is that throughout most of the interferometer both beams experience the same environment, – the relative phase of the two beams can change only in the measuring cavity. In other words, the reference and object beams are subject to the same temperature, pressure, vibration, etc. everywhere except in the cavity between the fiber tip and the specimen.

Figure 1 shows the entire experimental set-up schematically, including both the optics and the electronics. Within the photodetector, the current generated by the photodiode was amplified, converted to a voltage and fed directly into a standard ultrasonic signal processing system incorporating a high pass filter amplifier and a stepless gate. This latter component was used to select desired parts of the time varying signal to be routed to an oscilloscope or spectrum analyzer for evaluation. Except for the OFI system (laser, optics, optical fiber and custom wide band photodetector), most of the instrumentation used in these experiments was exactly the same as would be used in a typical study employing conventional ultrasonics.

Ultrasonic Experiments on Steel Test Bars

Initial tests to generate and detect Rayleigh waves were run using two standard piezoelectric transducers (with appropriate R-wave wedges) configured in the pitch-catch mode on the regularly machined (unpolished, flaw free) surface of a rectangular steel bar as shown in Figure 2. Figures 3a and 3b show characteristic time and frequency domain plots of the Rayleigh wave responses obtained with a transducer wedge-face to wedge-face separation of 50 mm. With a Rayleigh wave velocity, C_R, in steel of 2.96 mm/μs, the travel time between transducers would be approximately 17 μs. Since the actual time delay shown in Figure 3a was around 37 μs, the travel delay across the transducer wedges themselves must be around 20 μs, or 10 μs across each (since they are identical). In computing travel times in all subsequent experiments where the R-waves were generated using one of these transducer wedges and detected by the OFI, this 10 μs interval delay is subtracted from the measured times of

flight. The upper trace in Figure 3a shows a typical surface wave shape as detected by the piezoelectric transducer using an expanded time scale for the display. It can be seen from Figure 3b that the center frequency of the transducers is a little over 2 MHz when in contact with the surface of the specimen.

Similar tests were run on a flaw-free surface with the OFI used as a detector in place of the piezoelectric transducer, and comparable results were obtained. However, when a surface with a machined slot or "flaw" (as shown in Figure 4) was tested with piezoelectric transducer excitation and OFI detection, significant changes in the response were observed. Using a test configuration with the flaw located between the point of excitation and the OFI, the delay or "time-of-flight" of the R-wave observed in the oscilloscope trace would be seen to decrease as the OFI was moved towards the "flaw", exactly as expected. However, as the OFI was moved *past* the flaw, so that it was sensing at a point closer to the excitation than the flaw itself, Figure 4, the main R-wave signal increased markedly in amplitude, and *two additional* signals associated with components of the wave that had been reflected from the two ends of the flaw also appeared on the display. Figure 5a shows the time domain record for a typical test with the transducers in the locations shown in Figure 4. The trace in Figure 5a shows the ungated OFI signal transmitted to the oscilloscope through a high pass (>1 MHz) filter. The first peak, R_i, is the R-wave pulse generated by the piezoelectric transducer which was located 75 mm from the OFI. Using C_R = 2.96 mm/μs and adding the 10 μs delay in the excitation transducer predicts a total measured R-wave travel time of 35 μs – quite representative of the delay seen in the display. The next strong peak represents the partially reflected wave, R_1, from the top of the machined surface flaw which lies 18 mm beyond the OFI. This signal appears on the display almost 12 μs after R_i, as it should. The second reflection, R_2, is from the bottom of the slot. The R-wave has traveled down and back up the 2.8 mm long slot. This additional 5.6 μm travel distance accounts for the arrival of R_2 approximately 2 μs after R_1. The origins and paths of these waves are shown schematically in Figure 5b.

These results clearly demonstrate two major advantages of the OFI over conventional piezoelectric transducers. Firstly, because it does not involve the attachment of any energy absorbing mass to the surface at the point of measurement, OFI sensing does not itself in any way alter the acoustic wave. Consequently, the input and reflected waves may be monitored together. Secondly, the small sensing area of the OFI provides the high spatial resolution necessary for more accurate measurement of the time separation of closely spaced waves. This property is well illustrated by Figure 5a where the clearly discernable arrival times of waves R_1 and R_2 may be used to estimate the length of a flaw.

Next, in order to obtain frequency domain information, a series of tests were run in which the OFI signal was processed through the stepless gate directly to the spectrum analyzer, instead of the oscilloscope. Figure 6 shows a superposition of the spectra of the input wave, R_i, and the reflected wave, R_1, obtained from the gated responses recorded with the OFI positioned 15 mm in front of the flaw. The raw data sets from the analyzer were input to a personal computer where they were smoothed by boxcar averaging across five frequency readings. These results show a significant attenuation of some frequency components of the reflected wave centered around 1.8 MHz. There is additional attenuation at around 2.15 MHz and in the frequency band between 1.0 and 1.15 MHz. Since the flaw depth was greater than all but the largest significant acoustic wavelength components in the signal, most of these components are at least partially reflected by the flaw. However, components at frequencies that coincided with resonances of the free surface of the flaw are selectively attenuated. The strongest reflected frequency components appear at 1.5 MHz, which corresponds to a component wavelength, in steel, of nearly 2 mm. Since the depth of the flaw is around 2 mm, this should not be surprising. The attenuation in the reflected wave spectrum at around 2.15 MHz could be a second harmonic of the resonance at 1.07 MHz. It is interesting to note that this frequency represents an acoustic wavelength of around 2.8 mm, which is the length of the flaw.

In other words, the dominant features differentiating the reflected wave spectrum from the input wave spectrum are the strong deviations at wavelengths nearly identical to the depth and length of the surface flaw responsible for the reflection!

Similar analysis may be carried out for the transmitted wave signal obtained with the OFI positioned beyond the crack.

Optical Fiber Interferometer Improvements

While the OFI shows great potential as a superior detector/sensor for ultrasonic NDE, its deficiencies and limitations should be noted. The primary alignment deficiency of the single fiber configuration used in this work arises from the difficulty sometimes encountered in separating the return signal from the input end reflection, which is quite strong. Fortunately, this problem can be solved by replacing the beam splitter and single optical fiber with a 3 dB bidirectional optical fiber coupler. If the bidirectional coupler is configured, as most are, with two forward outputs, it would be necessary to terminate the unused fiber in such a way as to minimize the internally reflected return signal. This could be done most simply by immersing the end of the fiber in an index matching fluid. At the other end, either of the optical fibers might be used for the laser input and the photodetector, since the device is actually a 3 dB or half power beam divider. Preferably, such a coupler should be highly stable, which can best be assured by using a fused coupler design. Experiments by the authors successfully implementing such a coupler based OFI for acoustic wave measurement have recently been completed and will be described in a subsequent report.

Conclusions

It has been demonstrated that wide band OFI sensing can be a powerful tool of great potential for monitoring acoustic surface waves in steel, and likely many other important materials as well. Its point sensing and noncontact features permit the acquisition of considerably more information than can be obtained using a conventional piezoelectric transducer detector. Moreover, acousto-optic time-domain reflectometry and properly gated spectrum analysis have both been shown to be effective OFI signal evaluation techniques for the detection of surface flaws.

All of these experiments have been conducted using pulsed piezoelectric R-wave transducers to generate surface waves appropriate to the detection and evaluation of surface flaws. However, earlier work by the present authors [17] has also demonstrated that suitable acoustic waves may be generated by exciting a steel test bar with pulses of laser light guided through a noncontact optical fiber probe, and that such photonically generated acoustic waves may also be used to interrogate for flaws. The synthesis of these two fiber optic-based techniques for the excitation, interrogation and evaluation of materials and structures would provide a thermal-acousto-photonic (TAP) nondestructive evaluation capability with broad applications in many areas of reliability testing and certification. Moreover, whether used with conventional or fiber-optic based photo-acoustic wave excitation, OFI noncontacting sensors can readily be either (1) scanned across even complex surfaces or (2) configured in multiple sensor arrays to significantly enhance the interrogation and data gathering capabilities of TAP-NDE. Finally, since OFI sensors are flexible, compact and readily engineerable into robust, steerable probes, they provide a potential means of inspecting many important structures that would not otherwise be accessable because of geometry, complexity or scale.

Acknowledgments

The authors wish to thank AT&T Bell Laboratories, Texas A&M University, The University of Alabama in Huntsville and the U.S. Army Research Office under grant DAAL 03-86-K-0014 for their support of this effort. They also wish to express their thanks to R. O. Cook of Opto-Acoustic Sensors, Inc. for his custom wide band photoelectronics. One of the authors (B.R.P.) received a portion of his support from the American Society for Nondestructive Testing.

References

1. Calder, C. A. and Wilcox, W. W., "Noncontact Material Testing Using Laser Energy Deposition and Interferometry," *Materials Evaluation*, 86-91 (January 1980).
2. Lee, W. K. and Davis, C. C., "Laser Interferometric Studies of Laser-Induced Surface Heating and Deformation," *IEEE, J. of Quantum Electronics, QE-22*(4): 569-573 (April 1986).
3. Monchalin, J., "Optical Detection of Ultrasound at a Distance by Laser Interferometry," *11th World Conf. on Nondes. Testing*, Am. Soc. of NDT, Columbus, OH, 1017-1024 (1985).
4. Aharoni, A. and Jassby, K. M., "Monitoring Surface Properties of Solids by Laser Based SAW Time-of-Flight Measurements," *IEEE Trans. on Ultrasonics Ferroelectrics and Frequency Control, UFFC-33*(3): 250-256 (May 1986).
5. Birnbaum, G. and White, G. S., "Laser Techniques in NDE," *Res. Tech. in NDT*, Academic Press, London VII: 260-365 (1984).

6. Palmer, C. H., "Optical Probing of Acoustic Emission Waves," *Proc. 23rd Conf. Non-Destructive Evaluation of Materials*, Raquette Lake, NY, August 1976, Publ. by Plenum Press, New York, NY, 1979, pp. 347-378.
7. Green, R. E., Jr., "Some Innovative Techniques for Nondestructive Evaluation of Materials," *Novel NDE Methods for Materials (Proc. Conf.)*, Dallas, TX, 15-17 Feb. 1982, The Metallurgical Society/AIME, 1983, pp. 131-139.
8. Green, R. E., "Ultrasonic Materials Characterization," *Ultrasonics International 85*, Butterworth Scientific Ltd., 11-16 (1985).
9. Sciammarella, C. A., Asmadshani, M. A. and Subbaraman, B., "Holographic Interferometry Measurement of Ultrasonic Vibration Amplitudes," *Proc. 1986 Spring Meeting*, Soc. for Exp. Mech., New Orleans, LA, 706-710 (June 1986).
10. Djordjevic, B. B., Green, R. E., "High speed capture of acoustic emission and ultrasonic transients as detected with optical laser beam probes," *Proc. of the Ultrasonic International Conference*, Grav, Austria, 82-87 (1979).
11. Cook, R. O. and Hamm, C. W., "Fiber Optic Lever Displacement Transducer," *Appl. Optics, 18*(19): 3230-3241 (October 1979).
12. Culshaw, B., "Fiber Optic Sensing Techniques," *Res. Rech. in NDT*, Academic Press, London VII: 191-215 (1984).
13. Hogan, B. J., "Fiber-optic interferometer measures 10^{-9} cm displacement," *Design News*, 3(1): 62-63 (1972).
14. Wade, J. C., Zerwekh, P. S., Claus, R. O., "Detection of acoustic emission in composites by optical fiber interferometry," *Proc. of the 1981 IEEE Ultrasonics Symposium*, Chicago, Illinois (October 1981).
15. Ueha, S., Shibata, N., Tsujiuchi, J., "Flexible coherent optical probe for vibrational measurements," *Optical Communications*, 23(3): 407-409 (1977).
16. Drake, A. D. and Leiner, D. C., "Fiber-Optic Interferometer for Remote Subangstrom Vibration Measurement," *Rev. Sci. Instrum.*, 55(2): 162-165 (February 1984).
17. Burger, G. P., Dudderar, T. D., Gilbert, J. A., Peters, B. R. and Smith, J. A., "Laser Excitation Through Fiber Optics for NDE," *Journal of Nondestructive Evaluation*, 7(1): 57-64 (1987).

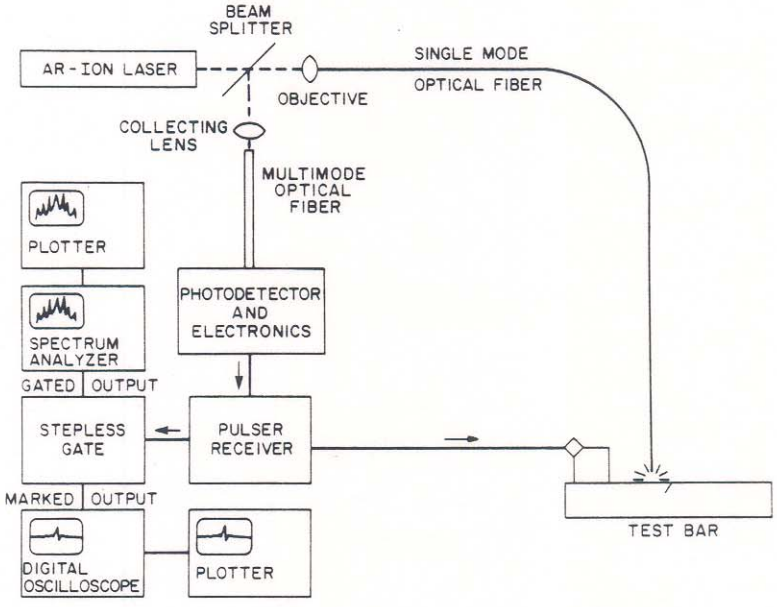

Fig. 1 Schematic of the Test Setup for the Conventional R-Wave Excitation and OFI Detection on a Steel Bar.

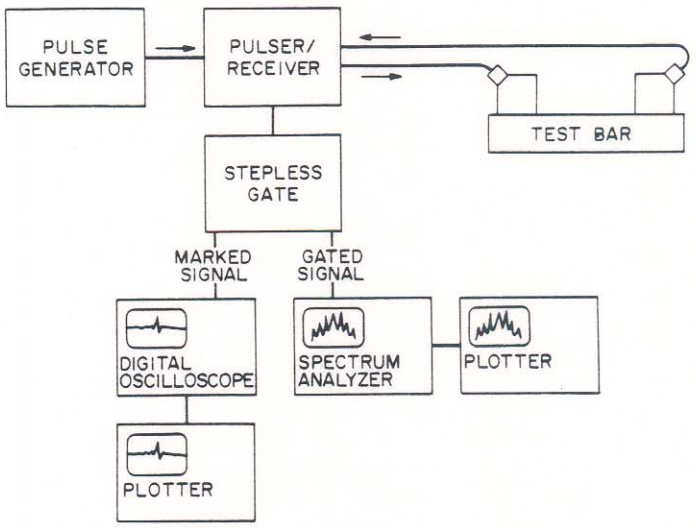

Fig. 2 Schematic of the Test Setup for a Conventional R-Wave Pitch-Catch Interrogation of a Steel Bar.

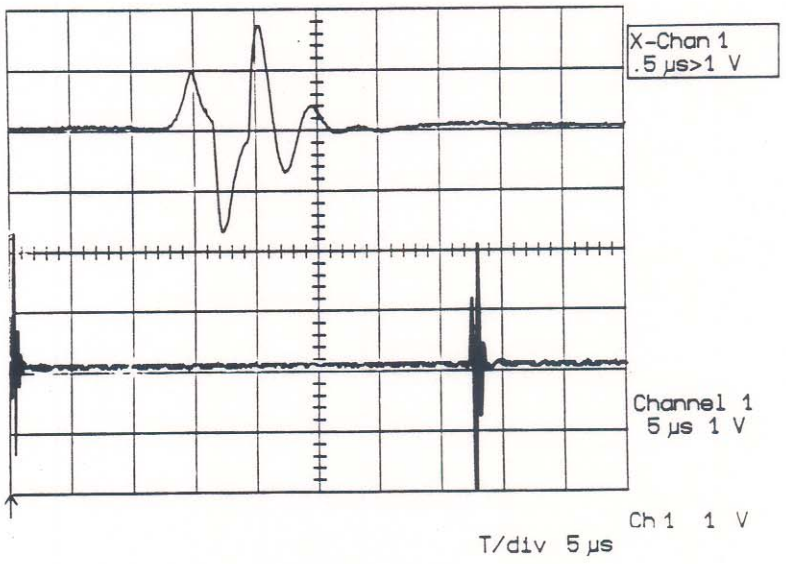

Fig. 3a Time Domain (Oscilloscope) Plots of an R-Wave Generated by Conventional Pitch-Catch on a Flaw Free Steel Bar Obtained Using Piezoelectric Transducers.

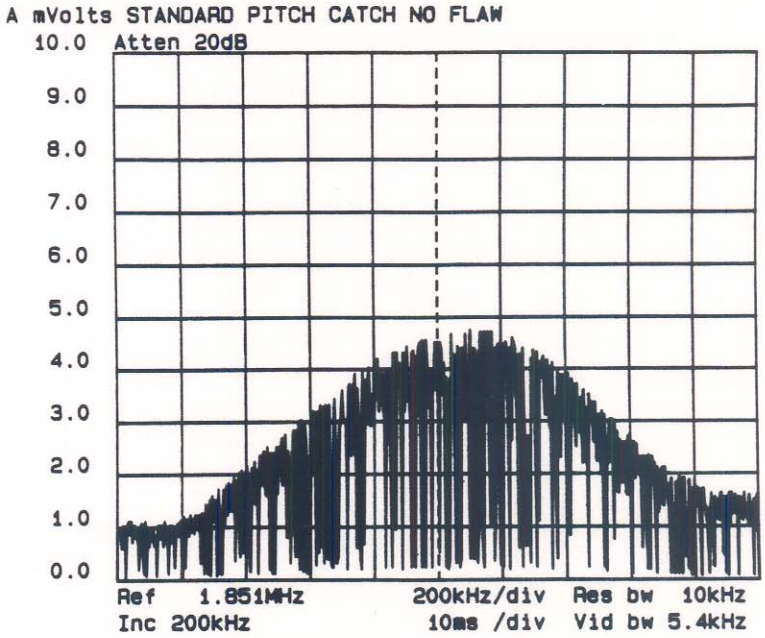

Fig. 3b Frequency Domain (Spectrum Analyzer) Plot of the R-Wave Shown in Figure 3a.

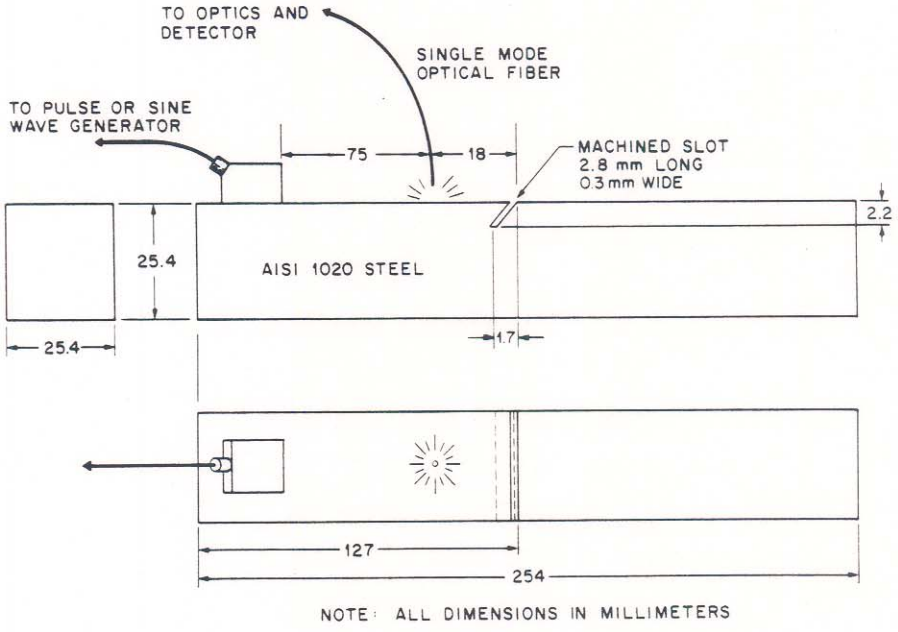

Fig. 4 Geometry and Instrumentation of the Steel Test Bar.

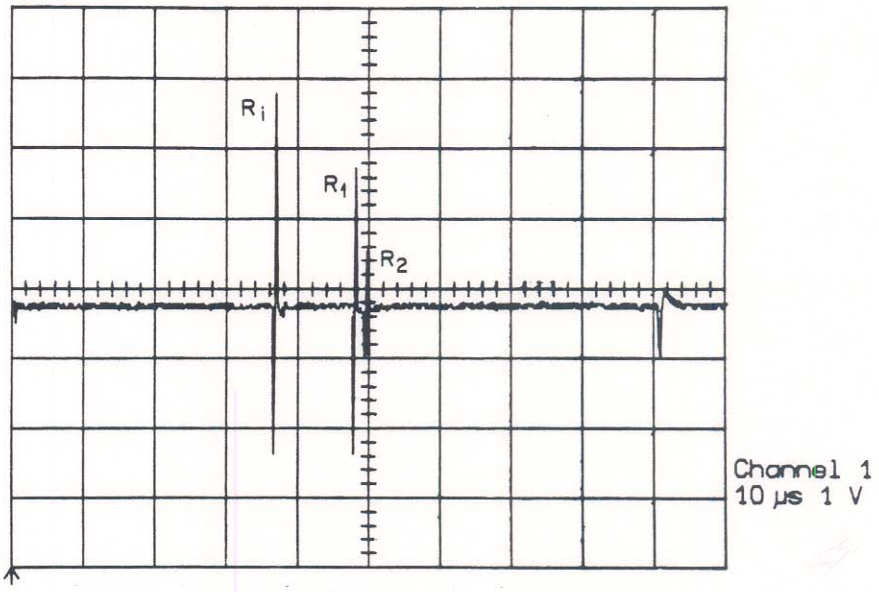

Fig. 5a Time Domain (Oscilloscope) Plot of the Input and Reflected R-Waves in a Flawed Steel Bar Obtained Using the OFI Sensor.

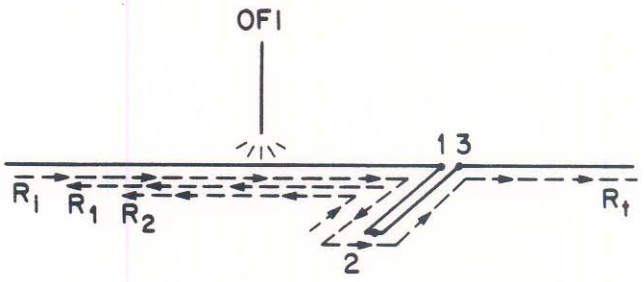

Fig. 5b Diagram Showing the Origins of the Various R-waves Detected by the OFI Sensor.

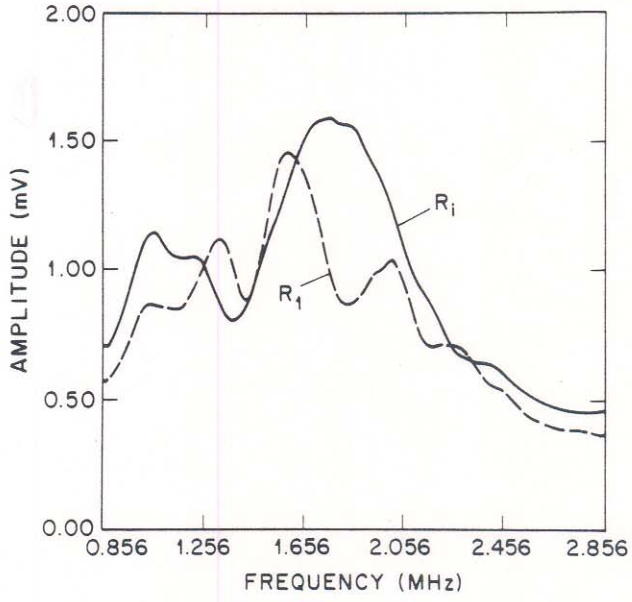

Fig. 6 Plots of the Digitized and Smoothed Frequency Spectra of the Input and Reflected R-Waves, R_i and R_1, in a Flawed Steel Bar.